



NEUROBIOLOGY

Neuronal-Specific Overexpression of a Mutant Valosin-Containing Protein Associated with IBMPFD Promotes Aberrant Ubiquitin and TDP-43 Accumulation and Cognitive Dysfunction in Transgenic Mice

Carlos J. Rodriguez-Ortiz,^{*} Hitomi Hoshino,^{*} David Cheng,^{†‡} Liqun Liu-Yescevitiz,^{§¶} Mathew Blurton-Jones,^{†‡} Benjamin Wolozin,^{§¶} Frank M. LaFerla,^{†‡} and Masashi Kitazawa^{*}

From the School of Natural Sciences,^{*} University of California, Merced, California; the Department of Neurobiology and Behavior[†] and the Institute for Memory Impairment and Neurological Diseases,[‡] University of California, Irvine, California; and the Departments of Pharmacology and Experimental Therapeutics[§] and Neurology,[¶] Boston University, Boston, Massachusetts

Accepted for publication
April 3, 2013.

Address correspondence to
Masashi Kitazawa, Ph.D.,
School of Natural Sciences,
University of California,
Merced, 394 Science and
Engineering, 5200 N. Lake Rd.,
Merced, CA 95343. E-mail:
mkitazawa@ucmerced.edu.

Mutations in valosin-containing protein (VCP) cause a rare, autosomal dominant disease called inclusion body myopathy associated with Paget disease of bone and frontotemporal dementia (IBMPFD). One-third of patients with IBMPFD develop frontotemporal dementia, characterized by an extensive neurodegeneration in the frontal and temporal lobes. Neuropathologic hallmarks include nuclear and cytosolic inclusions positive to ubiquitin and transactive response DNA-binding protein 43 (TDP-43) in neurons and glial activation in affected regions. However, the pathogenic mechanisms by which mutant VCP triggers neurodegeneration remain unknown. Herein, we generated a mouse model selectively overexpressing a human mutant VCP in neurons to study pathogenic mechanisms of mutant VCP-mediated neurodegeneration and cognitive impairment. The overexpression of VCP_{A232E} mutation in forebrain regions produced significant progressive impairments of cognitive function, including deficits in spatial memory, object recognition, and fear conditioning. Although overexpressed or endogenous VCP did not seem to focally aggregate inside neurons, TDP-43 and ubiquitin accumulated with age in transgenic mouse brains. TDP-43 was also found to co-localize with stress granules in the cytosolic compartment. Together with the appearance of high-molecular-weight TDP-43 in cytosolic fractions, these findings demonstrate the mislocalization and accumulation of abnormal TDP-43 in the cytosol of transgenic mice, which likely lead to an increase in cellular stress and cognitive impairment. Taken together, these results highlight an important pathologic link between VCP and cognition. (*Am J Pathol* 2013, 183: 504–515; <http://dx.doi.org/10.1016/j.ajpath.2013.04.014>)

Valosin-containing protein (VCP), a member of the type II adenosine triphosphatase associated with diverse cellular activities superfamily, is ubiquitous and is highly abundant in all cell types, including neurons.^{1–3} It forms a homohexameric structure and is involved in a variety of physiologic functions, including nuclear, endoplasmic reticulum, and Golgi membrane fusions; cell-cycle regulation; stress response-mediated apoptosis; B- and T-cell activation; transcriptional regulation; endoplasmic reticulum-associated protein degradation; and autophagosome maturation.^{4–9} Dysregulation of physiologic VCP function critically influences cell integrity and survival.

Mutations in VCP have been identified to cause a novel hereditary form of inclusion body myopathy associated with Paget disease of bone and frontotemporal dementia (IBMPFD).¹⁰ More recently, VCP mutations have been identified in a subset population of patients with amyotrophic lateral sclerosis (ALS).¹¹ Therefore, VCP mutations are hypothesized

Supported by NIH/National Institute of Arthritis and Musculoskeletal and Skin Diseases grant AR054695 (M.K.); partly by NIH grants P50AG16573 (F.M.L.), ES020395 (B.W.), NS066108 (B.W.), and NS073679 (B.W.); and by a grant from the American Health Assistance Foundation (B.W.).

to mediate as-yet-unknown mechanisms leading to skeletal muscle degeneration, bone deformation by osteoclast abnormality, and neurodegeneration. The penetrance of the disease phenotypes, however, varies among them. Approximately 30% of individuals with mutations develop frontotemporal dementia.^{10,12,13} Pathologically, neurons develop vacuoles, inclusions, and buildup of ubiquitinated proteins and transactive response DNA-binding protein (TDP-43) in cytoplasmic and nuclear compartments.^{14–16} No buildup of tau protein has been reported in patients, and the distribution of VCP seems unaltered in these neurons.¹⁷

Although VCP is involved in various critical cellular activities, key pathogenic mechanisms altered by the disease-relevant mutations are not well understood yet. To study the disease mechanisms and recapitulate the phenotypes, several *in vivo* models have been developed and reported. Recent studies by Taylor and colleagues¹⁶ demonstrated that overexpression of a disease-specific mutant VCP causes degeneration in muscle, bone, and neurons in a transgenic (Tg) mouse model. Mice with mutant VCP exhibit clearance of TDP-43 from the nuclear compartment and buildup of cytoplasmic TDP-43 co-localizing with ubiquitin.¹⁶ Similarly, Kimonis and colleagues¹⁸ generated a knock-in mouse model of IBMPFD, which expresses a disease-relevant VCP mutation (R155H) at physiologically relevant levels. In this model, increased cytoplasmic ubiquitin deposits were also evident in neurons together with increased levels of TDP-43 in brain tissue. These recent findings strongly suggest that mutant VCP promotes pathologic proteinopathies in the brain.

Several mechanisms have been proposed to explain how mutant VCP exerts its detrimental effects on the brain. Using transfection on the neuroblastoma cell line SH-SY5Y, Gitcho et al¹⁹ found that mutant VCP reduces proteasome activity and increases endoplasmic reticulum stress and apoptosis. Likewise, stable transfection of the activity-negative VCP mutant K524A leads to increased levels of the endoplasmic reticulum stress markers GRP78 and CHOP in differentiated PC12 cells.²⁰ Mutant VCP also promotes the accumulation of immature autophagic vesicles, suggesting that VCP is required for autophagosome maturation.⁸ In this regard, protein levels of the autophagy marker LC3/III have been reported to be increased in the brain as a consequence of mutations on VCP,¹⁸ and it is well documented that mutant VCP produces impaired autophagy in muscle cells.^{7,21,22}

We sought to investigate the underlying molecular mechanisms of the IBMPFD-associated mutant VCP in neurons. We, therefore, generated a Tg mouse model overexpressing mutant human VCP under the control of Thy1.2 promoter (Thy-VCP) to achieve forebrain-specific transgene expression. These mice exhibit an age-dependent decline in cognition and neuronal accumulation of cytoplasmic TDP-43. We also found that TDP-43 deposits co-localize with ubiquitin and accumulate in stress granules in Tg mice. High-molecular-weight TDP-43 was observed in the brain of mutant VCP—overexpressing mice and was localized exclusively in the cytoplasm. This observation may provide clues to

uncover key pathologic mechanisms of the disease and further validate the view that cytoplasmic TDP-43 accumulation is the culprit for mutant VCP—induced neurodegeneration. Taken together, this Tg line provides an additional *in vivo* model to study the cellular and molecular mechanisms that drive neural degeneration associated with IBMPFD.

Materials and Methods

Generation of Tg Mice

Human wild-type VCP was purchased from OriGene Technologies Inc. (Rockville, MD), and a disease-relevant VCP_{A232E} construct was generated by site-directed mutagenesis. The mutant VCP_{A232E} was then amplified by PCR (Phusion PCR kit; Cell Signaling Technology, Beverly, MA) and subcloned into the Thy1.2 expression cassette²³ using a homologous recombination-based approach (In-Fusion system; Clontech Laboratories, Mountain View, CA). The sequence-verified Thy1.2-VCP_{A232E} transgene was linearized by NotI and PvuI, purified, and microinjected into the pronuclei of single-cell embryos harvested from C57BL/6J mice by the University of California at Irvine Transgenic Mouse Facility (Irvine, CA).

Southern Blot and PCR Analyses of the Thy-VCP_{A232E} Transgene

All animal procedures and use were performed in strict accordance with NIH and University of California guidelines. All the mice used in this study were housed on a 12-hour light/dark schedule with *ad libitum* access to food and water. Tg mice were identified by tail DNA PCR genotyping and Southern blot analysis. For PCR genotyping, forward primer 5'-GAGGTATTCATCATGTGCT-3' and reverse primer 5'-AAGGACGATGCAAACAGCTT-3' (Figure 1A) liberated a 500-bp band from Tg mice (Figure 1C). Southern blot analysis was also performed to confirm the integrity of the transgene. Briefly, 2.5 kb of VCP cDNA was extracted by NheI and ClaI digestion and was used to make a probe for Southern blot analysis (Figure 1A). Ten micrograms of extracted tail DNA was digested overnight with EcoRI, NotI, and PvuI and was resolved overnight in 0.8% agarose gel. DNA was then denatured, transferred onto a nitrocellulose membrane, and probed with [P32]-CTP radiolabeled probe. The appearance of 4- and 5.5-kb bands on autoradiography indicated transgene-positive mice (Figure 1B).

Behavior Assays

Morris Water Maze

The protocol was conducted as previously described.²⁴ Briefly, mice were trained to swim to a 14-cm-diameter circular Plexiglas platform submerged 1.5 cm beneath the surface of the water and invisible to the mouse while swimming. The platform was fixed in place, equidistant from the

center of the tank and its walls. Mice were subjected to four training trials per day. During each trial, mice were placed into the tank at one of four designated start points in a pseudorandom order. Mice were trained for as many days as needed to reach the training criterion of 25 seconds (escape latency). If the mice failed to find the platform within 60 seconds, they were manually guided to the platform and were allowed to remain on it for 5 seconds. The probe was assessed 24 hours after the last training session and consisted of a 60-second trial without the platform. Escape latency on the probe trial was defined as the time taken by each animal to reach the area occupied by the platform during training. We also determined the number of times each animal completely crossed through the area occupied by the platform during training (platform crosses). Performance was monitored using the EthoVision XT version 7 video tracking software system (Noldus Information Technology Inc., Leesburg, VA). The numbers of mice used in the Morris water maze were as follows: 12 [6-month-old non-Tg (NT)], 12 (6-month-old A line), 11 (6-month-old B line), 12 (12-month-old NT), 10 (12-month-old A line), and 12 (12-month-old B line). These mice were also tested using the novel object recognition and contextual fear condition tests.

Novel Object Recognition

Each mouse was habituated to an empty Plexiglas arena (45 × 25 × 20 cm) for 3 consecutive days. On training (day 4), the mice were exposed to two identical objects placed at opposite ends of the arena for 5 minutes. Twenty-four hours later, the mice were allowed to explore one copy of the previously presented object (familiar) together with a new object for 5 minutes. A video camera was mounted above the arena, and all the sessions were recorded. Exploration was considered as pointing the head toward an object at a distance of <2.5 cm from the object, with its neck extended and vibrissae moving. Turning around, chewing, and sitting on the objects were not considered exploratory behaviors. The recognition index represents the percentage of the time that mice spend exploring the novel object. Mice that did not explore both objects during training were discarded from further analysis. Objects used in this task were carefully selected to prevent preference or phobic behaviors. To avoid olfactory cues, the objects were thoroughly cleaned with 70% ethanol and the sawdust was stirred after each trial.

Contextual Fear Conditioning

On training, mice were placed in the fear-conditioning chamber and were allowed to explore for 2 minutes before receiving three electric foot shocks (1 second, 0.2 mA; intershock interval, 2 minutes). Animals were returned to the home cage 30 seconds after the last foot shock. Twenty-four hours later, behavior in the conditioning chamber was video recorded for 5 minutes and subsequently was analyzed for freezing behavior, which was defined as the absence of all movement except for respiration.

Tissue Preparation

After deep anesthesia with sodium pentobarbital, the mice were perfused transcardially with 0.1 mol/L PBS, pH 7.4. Half the brain was fixed for 48 hours in PBS + 4% paraformaldehyde and then was cryoprotected in PBS + 30% sucrose for immunohistochemical and immunofluorescence analyses, and the other half was frozen in dry ice for biochemical analysis. Protein extracts were prepared by homogenizing whole brain hemisphere samples in 150 mg/mL of T-PER extraction buffer (Thermo Fisher Scientific Inc., Waltham, MA), complemented with protease and phosphatase inhibitors (Sigma-Aldrich, St. Louis, MO), and followed by centrifugation at $100,000 \times g$ for 1 hour. For nuclear-cytoplasmic fractionation, tissue was processed using the NE-PER kit (Thermo Fisher Scientific Inc.) following the manufacturer's instructions. For alkaline phosphatase treatment, 60 µg of protein was incubated with 60 U of bovine alkaline phosphatase (Sigma-Aldrich) at 37°C for 1 hour. Protein concentration was determined using the Bradford assay (Bio-Rad Laboratories, Hercules, CA). Unless noted otherwise, all Tg samples were from B line animals.

Immunohistochemical Analysis

Coronal free-floating sections (25 to 40 µm) were pretreated with 3% H₂O₂/10% methanol in Tris-buffered saline (TBS) for 30 minutes. After TBS washes, sections were incubated once in TBS + 0.1% Triton X-100 (TBST) for 15 minutes and once in TBST + 3% bovine serum albumin (BSA; Sigma-Aldrich) for 30 minutes and were blocked for 1 hour in TBS + 1% BSA + 5% goat serum (Vector Laboratories, Burlingame, CA). Sections were incubated overnight with VCP primary antibody (dilution 1:2000) (MA3-004; Pierce Biotechnology, Rockford, IL) in TBS + 1% BSA + 2% goat serum at 4°C. After washes, sections were incubated with biotinylated anti-mouse secondary antibody in TBS + 1% BSA + 2% goat serum at room temperature for 1 hour (dilution 1:500; Vector Laboratories), followed by development using Vectastain ABC kit and diaminobenzidine reagents (Vector Laboratories). Sections were mounted on gelatin-coated slides, dehydrated in graded ethanol series, cleared with xylenes, and coverslipped with DPX mounting medium (BDH Laboratory Supplies, Poole, UK). The specificity of the immune reactions was controlled by omitting the primary antibody.

Immunofluorescence

Coronal free-floating sections (25 to 40 µm) were pretreated with sodium citrate, 50 mmol/L (pH 6.0), for 10 minutes at 95°C and then were allowed to cool for half an hour. After TBS washes, sections were incubated once in TBST for 15 minutes and once in TBST + 3% BSA for 30 minutes and then were blocked for 1 hour in TBS + 1% BSA + 5% goat serum. Sections were incubated overnight with one or two

of the following primary antibodies: anti-TiA-1 (dilution 1:500) (ab2712; Abcam Inc., Cambridge, MA), TDP-43 (dilution 1:500) (12892-1-AP; Proteintech Group Inc., Chicago, IL), monoubiquitinated and polyubiquitinated proteins (dilution 1:500) (FK2; Enzo Life Sciences, Farmingdale, NY), PSD-95 (dilution 1:500) (ab18258; Abcam Inc.), and synaptophysin (dilution 1:200) (ab14692; Abcam Inc.) in TBS + 1% BSA + 2% goat serum at 4°C. After washes, sections were incubated with the appropriate secondary Alexa Fluor-conjugated antibody (dilution 1:200; Life Technologies Inc., Gaithersburg, MD) at room temperature for 1 hour, washed, and incubated with 300 nmol/L DAPI (Invitrogen, Carlsbad, CA) for 5 minutes. Sections were mounted onto gelatin-coated slides using Fluoromount-G (SouthernBiotech, Birmingham, AL) and were examined under an EVOS fl fluorescence microscope (Advanced Microscopy Group, Bothell, WA).

Semiquantitative analysis was performed using ImageJ software version 1.45s (NIH, Bethesda, MD). Nuclei were outlined and deleted from polyubiquitin or TiA-1 grayscale images; the rest was considered cytoplasmic staining. Images were converted to binary, and percentage of positive signal was computed from total image area. Three sections per animal were analyzed (5 to 6 mice per group).

For mean intensity measurements, three square regions of interest were defined on 16-bit grayscale images in the CA1 and CA3 regions, and mean pixel intensity was computed.

Immunoblotting

Equal amounts of protein were separated on 4% to 15% Bis-Tris gel and were transferred to polyvinylidene difluoride membranes. Membranes were blocked for 1 hour in TBS + 5% nonfat milk or Odyssey blocking solution (LI-COR Biosciences, Lincoln, NE). After blocking, membranes were incubated overnight with one or two of the following primary antibodies: TDP-43 (dilution 1:1000) (12892-1-AP; Proteintech Group Inc.), ubiquitin (dilution 1:3000) (Z0458; Dako, Carpinteria, CA), monoubiquitinated and polyubiquitinated proteins (dilution 1:1000) (FK2, Enzo Life Sciences), PSD-95 (dilution 1:1000) (ab18258; Abcam Inc.), synaptophysin (dilution 1:1000) (ab14692; Abcam Inc.), glyceraldehyde-3-phosphate dehydrogenase (dilution 1:5000) (FL-335; Santa Cruz Biotechnology, Santa Cruz, CA), p84 (dilution 1:1000) (5E10; Abcam Inc.), and tubulin (dilution 1:50,000) (B-5-1-2; Sigma-Aldrich) in TBS + 5% nonfat milk or Odyssey blocking solution + 0.2% Tween 20 at 4°C. After washes with TBS + 0.1% Tween 20, membranes were incubated for 1 hour with the specific secondary antibodies at a dilution of 1:5000 (horseradish peroxidase conjugated; Pierce Biotechnology) or 1:15000 (IRDye; LI-COR Biosciences) in TBS + 5% nonfat milk + 0.2% Tween 20 + 0.01% SDS. Blots were developed using SuperSignal (Thermo Fisher Scientific) or were scanned in an Odyssey infrared imager (LI-COR Biosciences). Image Studio software version 3.1.4 (LI-COR Biosciences) was used for protein quantification.

Sequential Extraction

Proteins from half the brain were extracted sequentially as described elsewhere.^{25,26} Briefly, brain tissue was first homogenized in low-salt (LS) buffer [10 mmol/L Tris, pH 7.5, 5 mmol/L EDTA, 1 mmol/L dithiothreitol, 10% sucrose, and protease/phosphatase inhibitor cocktails (Sigma-Aldrich)] and then was centrifuged at 25,000 × *g* for 30 minutes at 4°C to collect the LS fraction. Pellets were washed with PBS and were homogenized in high-salt buffer (LS + 1% Triton X-100 and 0.5 mol/L NaCl). The mixture was centrifuged at 180,000 × *g* for 30 minutes at 4°C, and the high-salt fraction was collected. The resulting pellets were washed with PBS and were homogenized in sarkosyl buffer (LS + 1% sarkosyl + 0.5 mol/L NaCl). The mixture was incubated for 1 hour at 22°C with gentle shaking followed by centrifugation at 180,000 × *g* for 30 minutes at 4°C. Sarkosyl-insoluble pellets were washed with PBS, resuspended in urea buffer (7 mol/L urea, 2 mol/L thiourea, 4% CHAPS, 30 mmol/L Tris, pH 8.5), and centrifuged at 25,000 × *g* for 30 minutes at 22°C. The protein concentration of each fraction was quantified by the Bradford assay (Bio-Rad Laboratories). Samples were mixed with 4× Laemmli loading buffer (Bio-Rad Laboratories) and 0.25 mol/L dithiothreitol, boiled for 10 minutes at 90°C, and loaded onto SDS gels as described previously herein.

Immunoprecipitation

Protein (150 μg) was precleaned for 1 hour with protein G-agarose (EMD Millipore Corporation, Billerica, MA) on a 360° rotator at 4°C. Beads were removed and samples were incubated with 1 μg of VCP antibody (MA3-004; Thermo Fisher Scientific) on a 360° rotator at 4°C. One hour later, protein G-agarose was added to samples and incubated for an additional 2 hours. Beads were washed several times, resuspended in 4× Laemmli loading buffer (Bio-Rad Laboratories) + 0.25 mol/L dithiothreitol, and boiled for 10 minutes. After centrifugation, supernatant was collected and analyzed by immunoblot.

SH-SY5Y Cell Transfection and Immunocytochemical Analysis

Cells were seeded at 70% confluency on chambered coverglass. Twenty-four hours later, 1 μg of one of the following constructs was transfected with BioT (Bioland Scientific, Paramount, CA) according to the manufacturer's instructions: human wild-type VCP, human VCP_{A232E}, or human VCP_{R155H} fused to enhanced green fluorescent protein. After 7 hours, the medium was replaced with fresh medium. Cells were processed for immunocytochemical analysis 72 hours after transfection. The VCP-enhanced green fluorescent protein plasmids used herein were a gift from Dr. Akira Kakizuka (Kyoto University, Kyoto, Japan).

For immunocytochemical analysis, cells were fixed in PBS + 4% paraformaldehyde (pH 7.4) for 15 minutes. After

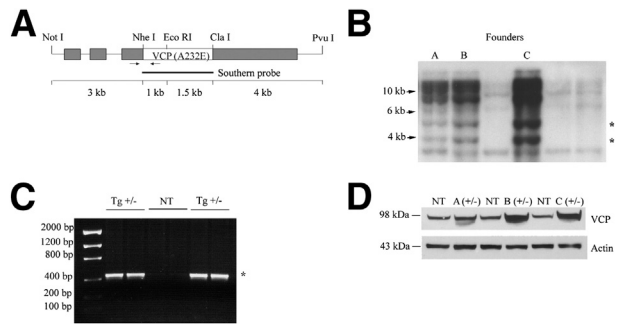


Figure 1 Generation of Thy-VCP_{A232E} Tg mice. **A:** The Thy1.2-VCP_{A232E} transgene construct shows the location of the sequence amplified by PCR genotyping (arrows; 0.5 kb) and the probe used in Southern blot analysis (2.5 kb). **B:** Southern blot analysis of founder lines A, B, and C. Asterisks indicate the 4- and 5.5-kb bands in Thy1.2-VCP_{A232E} Tg mice. Bands above 6 kb are undigested multiple copies of the transgene that were incorporated into genomic DNA. **C:** PCR genotyping shows amplification of 500 bp (asterisk) by the primer set shown as arrows in **A**. **D:** Immunoblot analysis of VCP in the brain. Increased steady-state levels of VCP at 98 kDa in the brain were detected in founder lines A, B, and C. Actin was used as loading control.

TBS washes, cells were incubated with TBST + 3% BSA for 10 minutes and were blocked in TBS + 1% BSA + 5% goat serum for 1 hour. Cells were incubated overnight with TDP-43 primary antibody (dilution 1:500) (12892-1-AP, Proteintech Group Inc.) in TBS + 1% BSA + 2% goat serum at 4°C. After washes, sections were incubated with Alexa Fluor-conjugated anti-rabbit secondary antibody in TBS + 1% BSA + 2% goat serum at room temperature for 1 hour (dilution 1:200; Life Technologies Inc.), washed, and incubated with 300 nmol/L DAPI for 5 minutes. Cells were coverslipped with Fluoromount-G (SouthernBiotech) and were examined under an EVOS fl fluorescence microscope (Advanced Microscopy Group). Semiquantitative analysis was performed using ImageJ software. Ten areas of each coverslip were selected (three independent experiments per group), and nuclei were outlined and deleted from TDP-43 grayscale images. Images were converted to binary, and the granule size and number were calculated on green fluorescent protein-positive cells.

Statistical Analysis

Comparisons between multiple groups used appropriate analysis of variance followed by Fisher post hoc tests. Comparisons between two groups used Student's *t*-test. $P \leq 0.05$ was considered significant.

Results

Forebrain Overexpression of Mutant VCP Impairs Cognitive Function in an Age-Dependent Manner

Mutant VCP_{A232E}-overexpressing mice were generated by microinjection of Thy1.2-VCP_{A232E} transgene into a single cell embryo from C57BL/6J mice. The Thy1.2 promoter

limited expression of the transgene to forebrain neurons.²⁷ Three founder lines were isolated showing integration of the Thy-VCP_{A232E} transgene. All the lines had the entire transgene successfully integrated into genomic DNA. The A line harbored the fewest copy numbers, whereas the B and C lines harbored approximately three to four times more copies of the transgene than the A line (Figure 1B). VCP expression was found to be higher on the brain of all Tg lines compared with their littermates (Figure 1D). Detailed genetic studies indicated that the C line founder was mosaic; hence, we excluded this line from further analysis.

Because transgene expression was limited to forebrain neurons, and high expression was observed in the hippocampus and cortex (Supplemental Figure S1J), a battery of behavioral tests, including the Morris water maze, novel object recognition, and contextual fear conditioning, was used to determine whether the expression of mutant VCP influences cognitive function in an age- and Tg dose-dependent manner (Figure 2). In the Morris water maze, the higher VCP-expressing B line showed significant impairment in acquisition at 6 and 12 months of age, whereas

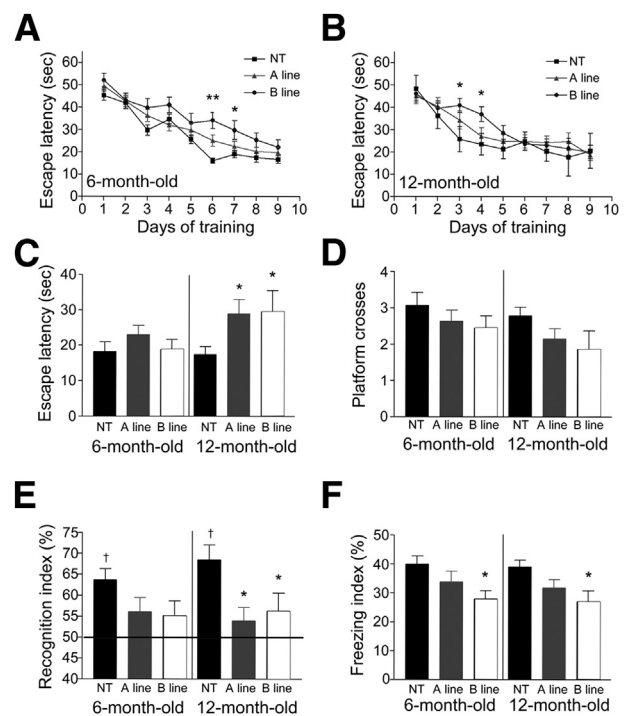


Figure 2 Overexpression of VCP_{A232E} causes age-dependent cognitive impairment. Six- and 12-month-old mice were trained in hippocampal- and cortical-dependent behavioral tasks. **A** and **B:** The higher-expressing VCP_{A232E} B line showed significant impairment in Morris water maze acquisition at 6 and 12 months of age, whereas the lower-expressing A line was not different from wild-type animals. **C** and **D:** Both 12-month-old Tg groups presented cognitive impairments when tested 24 hours later as measured by escape latency but not as measured by platform crosses. **E:** Both VCP_{A232E}-expressing lines performed poorly in the object recognition task at 12 months of age but not at 6 months of age. † $P < 0.05$ from 50% (chance level, shown as a horizontal line). **F:** Only the higher-expressing B line showed impairments at 6 and 12 months of age when contextual fear conditioning was assessed ($n = 10$ to 12 per group). * $P < 0.05$, ** $P < 0.01$. Data are given as means \pm SEM.

the lower VCP-expressing A line was not different from age-matched wild-type mice (Figure 2, A and B). However, both Tg lines were significantly impaired in memory retention, as measured by probe trial escape latency, at 12 months of age compared with NT mice (Figure 2C). The swim speed and swim distance in the defined timeframe were not

different between age-matched NT and Thy-VCP_{A232E} Tg mice (data not shown).

Similarly, object recognition showed that only 12-month-old Thy-VCP_{A232E} mice (A and B lines) were significantly impaired in recalling the familiar object, but 6-month-old Tg mice were not different from chance level (50% recognition index), although NT mice were different (Figure 2E). In contextual fear conditioning, only the higher-expressing B line showed impairments at 6 and 12 months of age (Figure 2F). The overexpression of mutant VCP in the forebrain, therefore, mediated age- and dose-dependent cognitive impairment in mice.

Mutant VCP Abets Focal TDP-43 Deposits that Co-Localize with Stress Granules and/or Ubiquitin in the Cortex

The overexpression of mutant VCP did not cause alterations in the gross anatomy of the hippocampus and cortex, where transgene expression driven by the Thy1.2 promoter was maximal (data not shown). Also, we did not observe any apparent aggregation or abnormal accumulation of endogenous VCP in neurons in these regions in NT mouse brain (Supplemental Figure S1, A–C). In Tg mice, however, VCP immunoreactivity was extended to dendrites in cortical and hippocampal regions, probably due to overexpression of mutant VCP (Supplemental Figure S1, D–I). A lack of VCP aggregate consisted of histopathologic observations on patients with IBMPFD.¹⁷ We next sought to examine whether TDP-43 immunoreactivity was altered in neurons. A previously reported Tg mouse model overexpressing mutant VCP exhibited complete clearance of TDP-43 from nuclear compartment and buildup of cytoplasmic TDP-43 deposits with ubiquitin.¹⁶ In the present mouse model, we observed abnormal accumulations of TDP-43 only, although a small percentage (19%), in neurons of Thy-VCP_{A232E} Tg mice but not in NT mice (Figure 3, C and D). Focal accumulation of TDP-43 was co-localized with stress granules, identified by TiA-1, in the cytoplasm (Figure 3, A and B). Quantification of 12- and 20-month-old cortical sections showed augmented levels of TiA-1 protein on 20-month-old Thy-VCP animals (Figure 3I). These findings support a redistribution of TDP-43 and increased stress responses, which may alter RNA metabolism and contribute to neurodegenerative processes. Similarly, a significantly increased number of Thy-VCP_{A232E} neurons had ubiquitin cytosolic inclusions (Figure 4, A and B), which were co-localized with cytoplasmic

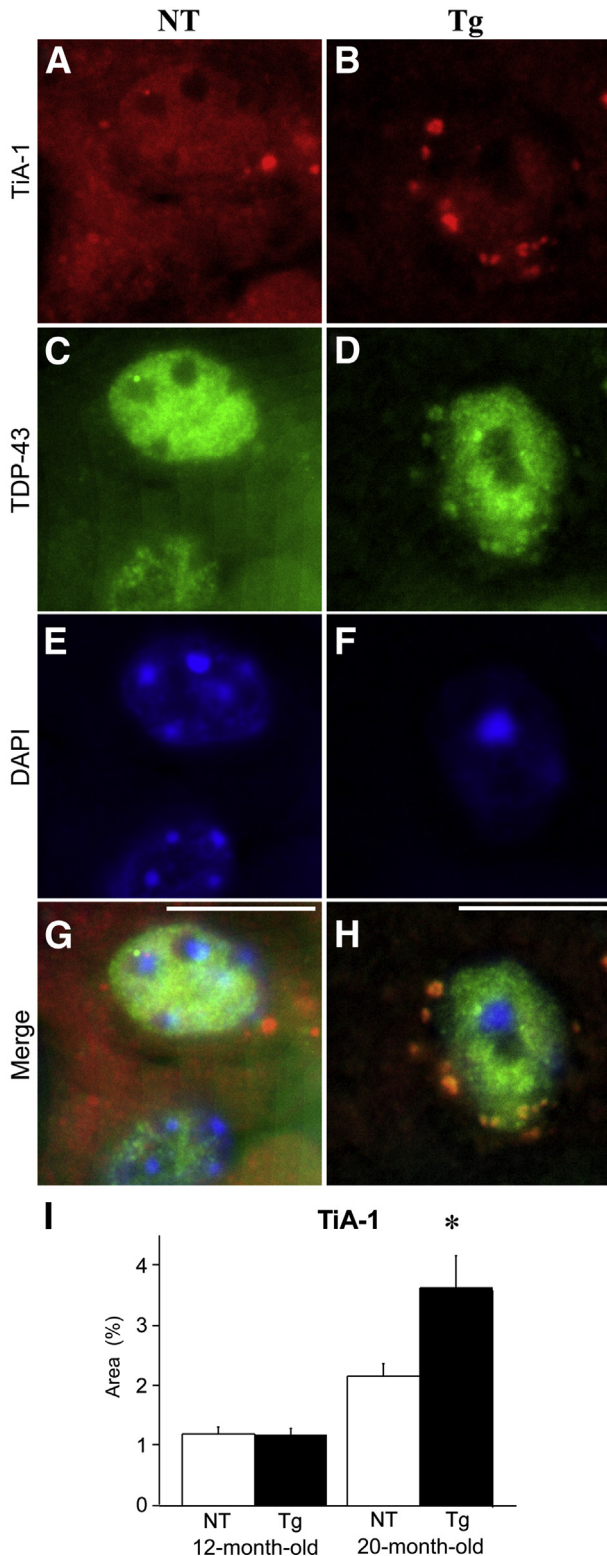


Figure 3 Thy-VCP_{A232E} mice display TDP-43 protein accumulation in the cytoplasm that co-localized with the stress granule marker TiA-1. **A and B:** Fluorescence microscopy analysis of 20-month-old mice revealed TiA-1 (red)—positive staining on wild-type (**A**) cortical sections but to a lesser degree than on VCP_{A232E} (**B**). **D:** TiA-1 co-localized with TDP-43 (green) deposits in the cytoplasm of Tg brains but not NT (**C**). **E and F:** DAPI staining (blue) was used as nuclear marker. **G and H:** Merge images of NT (**G**) and Tg (**H**). **I:** Quantification of 12- and 20-month-old sections showed significant increases in TiA-1 levels on the latter age. Data are given as means \pm SEM. Scale bars: 10 μ m. $n = 5$ to 6 per group. * $P < 0.05$.

TDP-43 aggregates (Figure 4, D and H). Accordingly, image analysis revealed that Thy-VCP_{A232E} brains have more ubiquitin-positive staining (Figure 4I). Biochemical analyses demonstrated accumulation of ubiquitinated proteins in an

age-dependent manner on Thy-VCP_{A232E} mice (Figure 4J). Ubiquitinated protein accumulation was detected to be greater in Thy-VCP_{A232E} brain cytoplasmic fractions (Figure 4, K and L).

TDP-43 Accumulates as a High-Molecular-Weight Form in the Thy-VCP_{A232E} Mouse Model

The underlying mechanisms by which TDP-43 is abnormally redistributed into cytoplasm and gains cytotoxicity remain unknown. Recent studies have suggested that TDP-43 is posttranslationally modified and abnormally accumulates in cells. Phosphorylation,²⁸ ubiquitination,^{25,29} and proteolytic cleavage³⁰ of TDP-43 are found to associate with various disease states. We, therefore, sought to investigate whether particular forms of TDP-43 predominantly accumulate in the cytoplasm of Thy-VCP_{A232E} Tg mice. We detected a high-molecular-weight (~90-kDa) TDP-43 band with greater intensity in aged B line Tg mice that corresponds to the size of dimeric TDP-43 (Figure 5A). Full-length TDP-43, on the other hand, was unchanged with age or transgene expression (Figure 5A). Nuclear-cytosolic fractionation showed a high-molecular-weight TDP-43 present only in the cytoplasm of Thy-VCP brain homogenates (Figure 5, B–E).

The aggregation states of TDP-43 were next determined by sequential extraction of brain tissue. We found several high-molecular-weight isoforms of TDP-43 in all fractions of Tg brain (Figure 6, A and B). A faint low-molecular-weight TDP-43 band (25 to 30 kDa), previously described in patients with ALS and frontotemporal dementia,²⁵ was also detected in detergent-soluble and sarkosyl fractions (Figure 6B). In addition, we observed increased levels of high-molecular-weight ubiquitinated proteins in LS and urea fractions (Figure 6C).

Tg-Specific High-Molecular-Weight TDP-43 Interacts with VCP

The overexpression of mutant VCP induced aberrant inclusions and redistribution of TDP-43 in forebrain neurons (Figures 3, 4, and 5). To determine whether VCP directly mediates these changes in TDP-43 through direct physical interaction, Thy-VCP_{A232E} and NT brain samples were immunoprecipitated with a VCP antibody and then were immunoblotted for TDP-

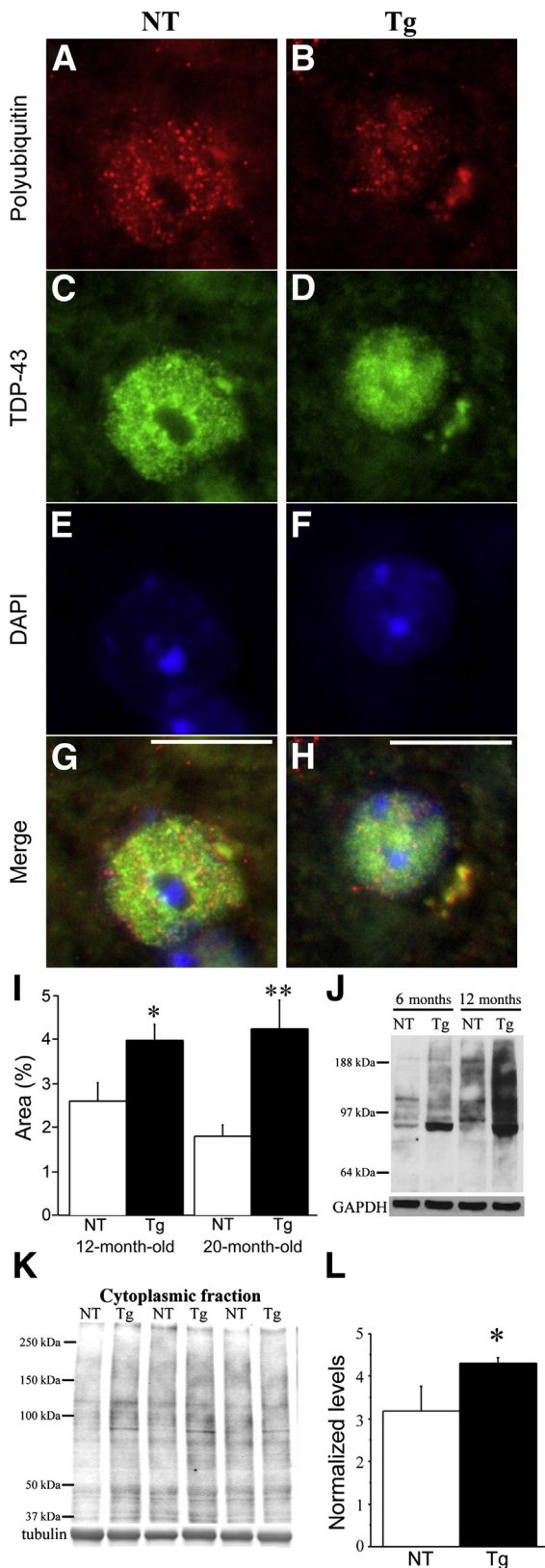


Figure 4 Thy-VCP_{A232E} mice show age-dependent cytosolic accumulation of polyubiquitinated proteins. **A–H:** VCP_{A232E} cortical sections from 20-month-old mice showed increased levels of polyubiquitin proteins (red) (**B**) and cytoplasmic TDP-43 (green) accumulation (**D**) compared with NT mice (**A** and **C**). **E** and **F:** DAPI staining (blue) was used as nuclear marker. **G** and **H:** Merge images of NT (**G**) and Tg (**H**). **I:** Quantification of 12- and 20-month-old sections uncovered increased levels of polyubiquitinated proteins on the Thy-VCP brain. **J:** Immunoblot analysis showed age-dependent buildup of polyubiquitinated proteins. Glyceraldehyde-3-phosphate dehydrogenase (GAPDH) was used as loading control. **K:** Polyubiquitinated proteins were accumulated in the cytosolic compartment of mutant VCP mice. Tubulin was used as loading control. **L:** Quantification of **K**. Scale bars: 10 μ m. $n = 5$ to 6 per group. * $P < 0.05$, ** $P < 0.01$. Data are given as means \pm SEM.

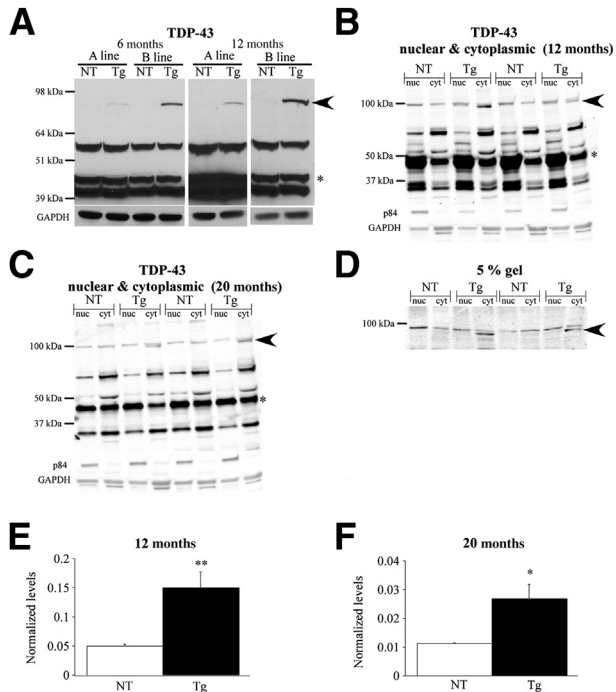


Figure 5 A high-molecular-weight TDP-43 isoform accumulates in the cytoplasm of Thy-VCP_{A232E} mice. **A:** Immunoblot analysis revealed a TDP-43 band of approximately 90 kDa only on mutant VCP mice at 6 and 12 months of age. Glyceraldehyde-3-phosphate dehydrogenase (GAPDH) was used as loading control. **B** and **C:** Nuclear-cytoplasmic fractionation unveiled a Tg-specific TDP-43 high-molecular-weight (HMW) band in the cytosol compartment of 12- and 20-month-old animals. p84 and GAPDH were used as nuclear and cytoplasmic purity controls, respectively. **D:** A better resolution of the TDP-43 HMW band was obtained when samples were run in a 5% acrylamide gel. **E** and **F:** Quantification of the HMW TDP-43 band in the cytoplasmic fraction of animals aged 12 (**E**) and 20 (**F**) months ($n = 6$ to 7 per group). * $P < 0.05$, ** $P < 0.01$. **Arrowheads** indicate HMW TDP-43 bands. **Asterisks** indicate full-length TDP-43 bands. Data are given as means \pm SEM.

43. We found that only high-molecular-weight TDP-43 was immunoprecipitated with VCP (Figure 7A).

To determine whether high-molecular-weight TDP-43 is a hyperphosphorylated isoform, Tg and NT brain samples were treated with alkaline phosphatase and were analyzed by Western blot. Alkaline phosphatase treatment did not reduce high-molecular-weight TDP-43 levels (Figure 7, B and C). Together, these data suggest a physical interaction between VCP and a high-molecular-weight TDP-43 isoform in Tg mice.

Mutant VCP Overexpression Does Not Show Evident Neurodegeneration

As shown in Figure 2, forebrain neuron-specific expression of mutant VCP exhibited age- and dose-dependent cognitive impairment in mice. We sought to investigate whether loss of synapses contributed to cognitive impairment in Thy-VCP_{A232E} Tg mice. Both synaptophysin and PSD-95 in the hippocampus were quantitatively measured by immunoblots (Supplemental Figure S2, A and B, for synaptophysin and Supplemental Figure S2, C and D, for PSD-95), but no

definitive differences were detected. Similarly, immunofluorescence staining failed to show any statistical significance in the intensity of synaptophysin (Supplemental Figure S2, E and F) or PSD-95 (Supplemental Figure S2, G and H) in VCP Tg mice compared with age-matched NT mice.

It has been proposed that mutant VCP leads to increased NF- κ B signaling, producing degeneration of muscle and bone tissue through hyperactivity of the NF- κ B pathway.^{16,31} VCP modulates the NF- κ B signaling cascade by regulating the degradation of I κ B- α , which, in turn, frees NF- κ B from an inactive to a phosphorylated active conformation that translocates to the nucleus. In this regard, it was shown that myoblast C2C12 cells overexpressing mutant VCP present lower I κ B- α protein levels and increased phosphorylated NF- κ B protein levels compared with cells overexpressing wild-type VCP when stimulated with tumor necrosis factor α .¹⁶ To address whether altered NF- κ B signaling underlies cognitive impairment in Thy-VCP_{A232E} mice, we analyzed NF- κ B and I κ B protein levels in the nuclear and cytoplasmic fractions of wild-type and Tg animals (Supplemental Figure S3, A–E) and the activity of NF- κ B by electrophoretic mobility shift assay (Supplemental Figure S3F), but we did not uncover differences between genotypes (Supplemental Figure S3). However, we observed that a small number of neurons exhibited nuclear localization of NF- κ B in VCP Tg mice (Supplemental Figure S3G). Further studies are required to identify the link between VCP, TDP-43, and cognitive impairment in the brain.

SH-SY5Y Cells Transfected with Mutant VCP Present TDP-43 Cytoplasmic Inclusions

To evaluate VCP-mediated TDP-43 accumulation in the cytoplasm in a cell culture model, human neuroblastoma

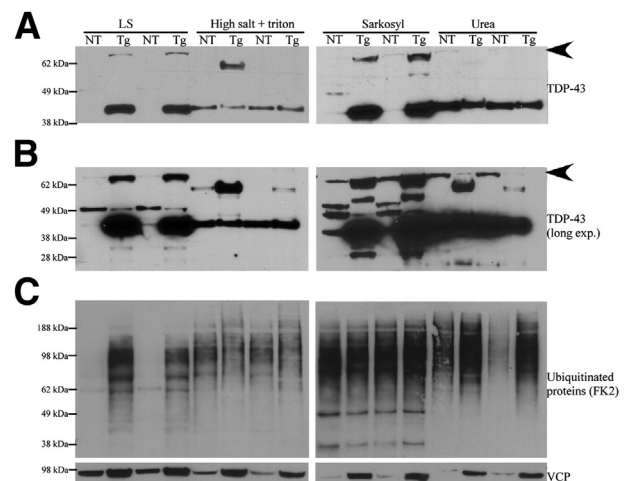


Figure 6 High-molecular-weight TDP-43 is present in different aggregation states. **A** and **B:** Sequential extraction of brain tissue showed high-molecular-weight TDP-43 (**arrowheads**) in detergent-soluble and detergent-insoluble fractions. **C:** High-molecular-weight ubiquitinated proteins were detected in LS and urea fractions ($n = 6$ per group).

SH-SY5Y cells were transfected with one of the following constructs: wild-type VCP, VCP_{R155H}, or VCP_{A232E} fused to enhanced green fluorescent protein. Seventy-two hours after transfection, analysis of green fluorescent protein-positive cells indicated formation of a small number of TDP-43 inclusions in the cytoplasm when IBMPFD-related VCP mutations were introduced (Figure 8, A–F). Larger TDP-43 deposits were observed in the cytosol of VCP_{A232E}- and VCP_{R155H}-transfected cells compared with transfection with wild-type VCP (Figure 8M).

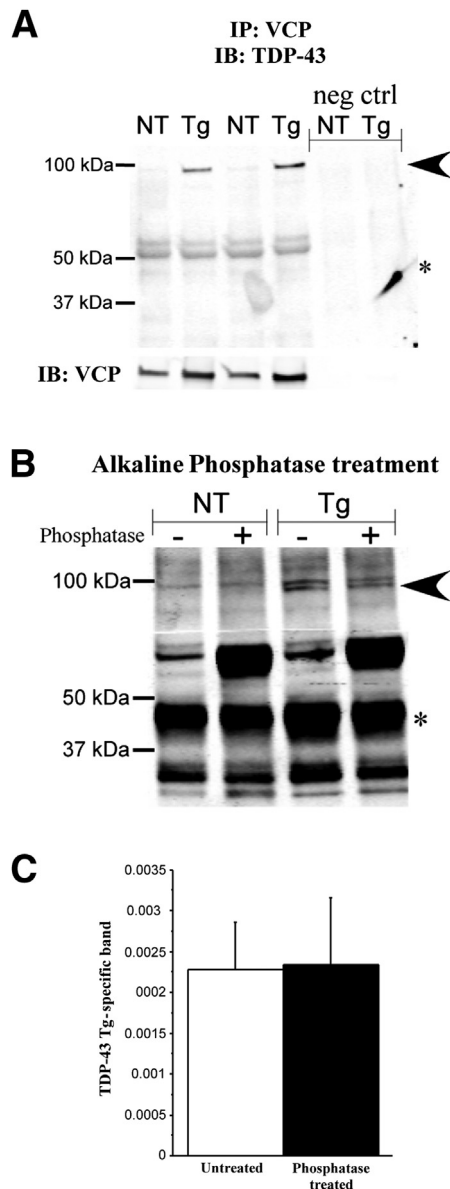


Figure 7 High-molecular-weight TDP-43 interacts with VCP. **A:** Immunoprecipitation (IP) with a VCP antibody and immunoblot (IB) for TDP-43 uncovered an interaction between VCP and the Tg-specific TDP-43 high-molecular-weight isoform (arrowhead). **B:** High-molecular-weight TDP-43 is not affected by alkaline phosphatase treatment (arrowhead). **C:** Quantification of **B** ($n = 4$ per group). Asterisks indicate full-length TDP-43 bands. Data are given as means \pm SEM.

Discussion

TDP-43 is a DNA- and RNA-binding protein and a component of heterogeneous nuclear ribonucleoproteins, which are involved in RNA transcription, splicing, and transport.^{32,33} In particular, because TDP-43 has nuclear localizing signal and nuclear export signal in its sequence along with two DNA/RNA recognition motifs (RRM1 and RRM2),³⁴ it is critically involved in the trafficking of mRNAs between the nucleus and cytosol.^{35,36} Although TDP-43 is predominantly localized in the nuclear compartment, its physiologic role in spines and involvement in synaptic plasticity have recently been reported,³⁵ further suggesting a diverse role of TDP-43 in neurons. Shortly after abnormal TDP-43 was first recognized as forming a part of cytosolic inclusions in affected neurons in ALS and frontotemporal dementia,²⁵ mutations on TDP-43 causing ALS were identified,^{37,38} confirming that TDP-43 plays a critical and causal role in the pathogenesis of ALS.

Redistribution and accumulation of TDP-43 in the cytosol are also observed in affected skeletal muscle fibers in inclusion body myositis,¹⁴ suggesting that TDP-43 may be a primary culprit in various human diseases in multiple tissues. In some cases, TDP-43 is reported to co-localize with ubiquitin or stress granules.^{39–41} In Tg mice and cell culture models, increased cytosolic accumulation of TDP-43 or its proteolytic 25-kDa fragment triggers neurotoxicity.^{42,43} However, detailed molecular mechanisms by which cytosolic TDP-43 induces cell death have not yet been defined.

Some biochemical evidence suggests that TDP-43 forms a homodimer in physiologic conditions.³⁴ In addition, structural analysis of the TDP-43 RRM2 domain showed similar structural arrangement to heterogeneous nuclear ribonucleoprotein A1 protein, which forms a homodimer when bound to DNA.³⁴ In this study, it was also revealed that dimeric RRM2 is quite resistant to temperature because of a highly stable antiparallel β -sheet conformation, presenting a denaturing temperature of approximately 85°C. On the other hand, a TDP-43 fragment that included both RRM domains of TDP-43 protein showed a much lower melting point (approximately 50°C). In the present report, we observed a high-molecular-weight TDP-43 that is consistent with the size of dimeric TDP-43, exclusively expressed in the cytoplasm of Tg mice. This putative dimeric TDP-43 band would also be in a thermal-stable conformation, as well as resistant to denaturing and reducing conditions (Figure 5). In this regard, Shiina et al⁴⁴ reported an 86-kDa cytoplasmic TDP-43 isoform in several human cell lines. The 86-kDa band reacts to specific N-terminal and C-terminal TDP-43 antibodies and is sensitive to siRNA targeted to TDP-43. Moreover, samples treated with dithiothreitol or 2-mercaptoethanol before immunoblotting showed the 86-kDa band when immunoblotted with TDP-43 antibodies. These authors detected a similar molecular-weight band in detergent-soluble brain samples from patients with disparate affections, including ALS, parkinsonism, multiple sclerosis, schizophrenia, and depression.⁴⁴ When this 86-kDa isoform was overexpressed in cell culture, it promoted

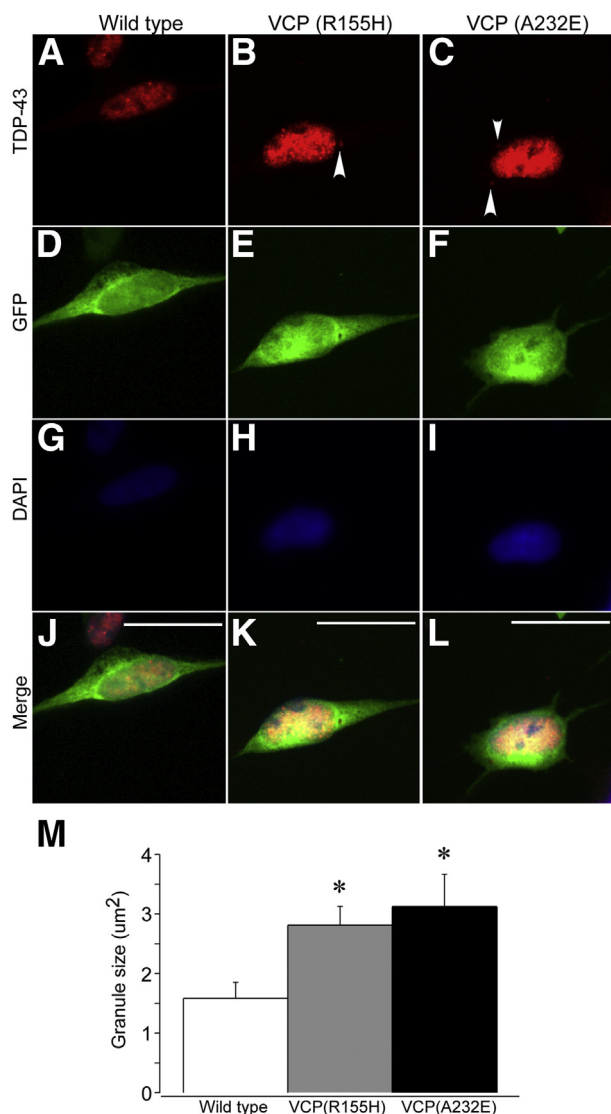


Figure 8 SHSY-5Y neuroblastoma cells present TDP-43 cytosolic buildup when transfected with mutant VCP. Cells transfected with wild-type VCP showed TDP-43 (red)—positive staining mainly in the nucleus, with little to no cytoplasmic signal (**A**). Cells transfected with the common R155H (**B**) or severe A232E (**C**) VCP mutation also showed TDP-43 nuclear signal with small, but evident, TDP-43 deposits in the cytoplasm (**arrowheads**). **D–F**: Green fluorescence protein signal was used to identify transfected cells. **G–I**: DAPI staining (blue) was used as nuclear marker. **J–L**: Merge images of wild-type VCP, VCP(R155H), and VCP(A232E), respectively. **M**: TDP-43 granule size was larger in cells transfected with mutant VCP. Scale bars: 50 µm. * $P < 0.05$. Data are given as means \pm SEM.

the accumulation of TDP-43—reactive proteins that range in size from 70 to 200 kDa, indicating that dimeric TDP-43 would be a seed molecule for TDP-43 inclusions.⁴⁴

VCP is involved in multiple cellular functions through interaction with a plethora of cofactors. For example, VCP associates with several E3 ligases to deliver polyubiquitinated proteins to the proteasome for degradation.^{45,46} In addition, several polyubiquitinated proteins require direct interaction with the N-terminal region of VCP to translocate to the proteasome.⁴⁷ Accordingly, mutant VCP isoforms lead to altered

proteasome activity and induce apoptosis.^{17,19} A previous report showed interaction between VCP and TDP-43 in ALS brain samples and SHSY-5Y cells transfected with mutant VCP.¹⁹ Herein, we observed interaction between VCP and TDP-43 in the Thy-VCP mouse; however, VCP coupled exclusively to the putative TDP-43 homodimer, probably to direct it to the proteasome for degradation, but when this process is disrupted by mutant VCP, TDP-43 accumulates in the cytoplasm. In support of this view, it has been reported that IBMPFD-relevant VCP mutations cause cytoplasmic TDP-43 inclusions *in vitro*.¹⁹

Furthermore, some evidence indicates that TDP-43 is degraded through the ubiquitin-proteasome system and that impairment of the proteasome leads to aggregation of ubiquitinated TDP-43 in the cytoplasm.^{19,48,49} Herein, we observed VCP_{A232E}-mediated accumulation of TDP-43 in the cytoplasm specifically concentrated in stress granules. In response to stress insults, cells sequester nonessential RNA transcripts in protein-mRNA complexes called stress granules, allowing available resources to deal with stress. Protein-mRNA complex formation relies on regulated aggregation of RNA-binding proteins, such as TDP-43.⁵⁰ In this regard, it has been shown that cellular stress produces TDP-43 recruitment to stress granules^{40,41} and that TDP-43 is involved in stress granule assembly and maintenance.⁵¹ Consistently, TDP-43 regulates the maturation of stress granules containing G3BP and co-localizes with stress granules containing TiA-1.^{51,52} These pieces of evidence indicate that regulated protein aggregation of TDP-43, similar to other RNA-binding proteins, exerts direct influence on stress granule dynamics and the way cells deal with stress.⁵⁰

In physiologic conditions, stress granules rapidly dissociate when stress is overcome. However, mutations on key proteins of the stress granules pathway and/or chronic stress may lead to up-regulation of stress granule formation and, consequently, pathologic aggregation of proteins.⁵⁰ Accordingly, ALS-relevant TDP-43 mutations have been reported to produce larger stress granules than their wild-type counterpart,^{41,53} which may be an indication of an altered stress response or an increased propensity for aggregation. It has also been shown that TDP-43 accumulation in stress granules can progress to stable cytosolic aggregates that may be part of a toxic gain-of-function process.⁵⁴ Therefore, manipulation of the pathways involved in stress granule formation provides an opportunity to modify the pathologic protein aggregation commonly observed in neurodegenerative diseases.⁵⁰

Another interesting and related mechanism by which TDP-43 may contribute to pathologic abnormality is derived from the fact that TDP-43 is required for activity-dependent transport and stability of mRNAs in dendrites.³⁵ Pathologic TDP-43 relocalization to stress granules may impair local dendritic mRNA translation in response to neuronal activity, contributing to neurodegeneration through the disruption of normal synaptic function.

We generated a Tg mouse overexpressing an IBMPFD-associated mutant VCP selectively in forebrain neurons to

investigate the molecular and cellular mechanisms by which mutant VCP mediates neuronal dysfunction and neurodegeneration. Although extensive neurodegeneration was not observed throughout the life span of mice, age-dependent cognitive decline, increased stress response, and altered TDP-43 distribution in affected brain regions were clearly detected in Thy-VCP_{A232E} mice. Previous Tg models have successfully recapitulated different IBMPFD phenotypes, contributing valuable insights on IBMPFD disease mechanisms.^{15,16,18,42,55} The present Tg mouse model exhibited several remarkable changes in affected neurons, including accumulation of high-molecular-weight TDP-43 only in the cytosolic compartment with age. This model could serve as an additional *in vivo* tool to further study the brain abnormalities associated with IBMPFD and other TDP-43 proteinopathies without confounding complications, such as myopathy and bone deformations, that could interfere with cognitive assessments.

Supplemental Data

Supplemental material for this article can be found at <http://dx.doi.org/10.1016/j.ajpath.2013.04.014>.

References

- Muller JM, Meyer HH, Ruhrberg C, Stamp GW, Warren G, Shima DT: The mouse p97 (CDC48) gene: genomic structure, definition of transcriptional regulatory sequences, gene expression, and characterization of a pseudogene. *J Biol Chem* 1999, 274:10154–10162
- Hirabayashi M, Inoue K, Tanaka K, Nakadate K, Ohsawa Y, Kamei Y, Popiel AH, Sinojima A, Iwamatsu A, Kimura Y, Uchiyama Y, Hori S, Kakizuka A: VCP/p97 in abnormal protein aggregates, cytoplasmic vacuoles, and cell death, phenotypes relevant to neurodegeneration. *Cell Death Differ* 2001, 8:977–984
- Zalk R, Shoshan-Barmatz V: ATP-binding sites in brain p97/VCP (valosin-containing protein), a multifunctional AAA ATPase. *Biochem J* 2003, 374:473–480
- Wang Q, Song C, Li CC: Hexamerization of p97-VCP is promoted by ATP binding to the D1 domain and required for ATPase and biological activities. *Biochem Biophys Res Commun* 2003, 300:253–260
- Wang Q, Song C, Li CC: Molecular perspectives on p97-VCP: progress in understanding its structure and diverse biological functions. *J Struct Biol* 2004, 146:44–57
- Zhang H, Wang Q, Kajino K, Greene MI: VCP, a weak ATPase involved in multiple cellular events, interacts physically with BRCA1 in the nucleus of living cells. *DNA Cell Biol* 2000, 19:253–263
- Ju JS, Fuentelba RA, Miller SE, Jackson E, Pivnick-Worms D, Baloh RH, Weihl CC: Valosin-containing protein (VCP) is required for autophagy and is disrupted in VCP disease. *J Cell Biol* 2009, 187:875–888
- Tresse E, Salomons FA, Vesa J, Bott LC, Kimonis V, Yao TP, Dantuma NP, Taylor JP: VCP/p97 is essential for maturation of ubiquitin-containing autophagosomes and this function is impaired by mutations that cause IBMPFD. *Autophagy* 2010, 6:217–227
- Wojcik C, Yano M, DeMartino GN: RNA interference of valosin-containing protein (VCP/p97) reveals multiple cellular roles linked to ubiquitin/proteasome-dependent proteolysis. *J Cell Sci* 2004, 117:281–292
- Watts GD, Wymer J, Kovach MJ, Mehta SG, Mumm S, Darvish D, Pestronk A, Whyte MP, Kimonis VE: Inclusion body myopathy associated with Paget disease of bone and frontotemporal dementia is caused by mutant valosin-containing protein. *Nat Genet* 2004, 36:377–381
- Johnson JO, Mandrioli J, Benatar M, Abramzon Y, Van Deerlin VM, Trojanowski JQ, et al: Exome sequencing reveals VCP mutations as a cause of familial ALS. *Neuron* 2010, 68:857–864
- Kovach MJ, Waggoner B, Leal SM, Gelber D, Khardori R, Levenstien MA, Shanks CA, Gregg G, Al-Lozi MT, Miller T, Rakowicz W, Lopate G, Florence J, Glosser G, Simmons Z, Morris JC, Whyte MP, Pestronk A, Kimonis VE: Clinical delineation and localization to chromosome 9p13.3-p12 of a unique dominant disorder in four families: hereditary inclusion body myopathy: Paget disease of bone, and frontotemporal dementia. *Mol Genet Metab* 2001, 74:458–475
- Kimonis VE, Fulchiero E, Vesa J, Watts G: VCP disease associated with myopathy: Paget disease of bone and frontotemporal dementia: review of a unique disorder. *Biochim Biophys Acta* 2008, 1782:744–748
- Salajegheh M, Pinkus JL, Taylor JP, Amato AA, Nazareno R, Baloh RH, Greenberg SA: Sarcoplasmic redistribution of nuclear TDP-43 in inclusion body myositis. *Muscle Nerve* 2009, 40:19–31
- Badadani M, Nalbandian A, Watts GD, Vesa J, Kitazawa M, Su H, Tanaja J, Dec E, Wallace DC, Mukherjee J, Caiizzo V, Warman M, Kimonis VE: VCP associated inclusion body myopathy and paget disease of bone knock-in mouse model exhibits tissue pathology typical of human disease. *PLoS One* 2010, 5:e13183
- Custer SK, Neumann M, Lu H, Wright AC, Taylor JP: Transgenic mice expressing mutant forms VCP/p97 recapitulate the full spectrum of IBMPFD including degeneration in muscle, brain and bone. *Hum Mol Genet* 2010, 19:1741–1755
- Forman MS, Mackenzie IR, Cairns NJ, Swanson E, Boyer PJ, Drachman DA, Jhaveri BS, Karlawish JH, Pestronk A, Smith TW, Tu PH, Watts GD, Markesbery WR, Smith CD, Kimonis VE: Novel ubiquitin neuropathology in frontotemporal dementia with valosin-containing protein gene mutations. *J Neuropathol Exp Neurol* 2006, 65:571–581
- Nalbandian A, Llewellyn KJ, Kitazawa M, Yin HZ, Badadani M, Khanlou N, Edwards R, Nguyen C, Mukherjee J, Mozaffar T, Watts G, Weiss J, Kimonis VE: The homozygote VCP(R155H/R155H) mouse model exhibits accelerated human VCP-associated disease pathology. *PLoS One* 2012, 7:e46308
- Gitcho MA, Strider J, Carter D, Taylor-Reinwald L, Forman MS, Goate AM, Cairns NJ: VCP mutations causing frontotemporal lobar degeneration disrupt localization of TDP-43 and induce cell death. *J Biol Chem* 2009, 284:12384–12398
- Kobayashi T, Tanaka K, Inoue K, Kakizuka A: Functional ATPase activity of p97/valosin-containing protein (VCP) is required for the quality control of endoplasmic reticulum in neuronally differentiated mammalian PC12 cells. *J Biol Chem* 2002, 277:47358–47365
- Vesa J, Su H, Watts GD, Krause S, Walter MC, Martin B, Smith C, Wallace DC, Kimonis VE: Valosin containing protein associated inclusion body myopathy: abnormal vacuolization, autophagy and cell fusion in myoblasts. *Neuromuscul Disord* 2009, 19:766–772
- Ju JS, Weihl CC: Inclusion body myopathy: Paget's disease of the bone and fronto-temporal dementia: a disorder of autophagy. *Hum Mol Genet* 2010, 19:R38–R45
- Oddo S, Caccamo A, Shepherd JD, Murphy MP, Golde TE, Kaye R, Metherate R, Mattson MP, Akbari Y, LaFerla FM: Triple-transgenic model of Alzheimer's disease with plaques and tangles: intracellular Abeta and synaptic dysfunction. *Neuron* 2003, 39:409–421
- Billings LM, Oddo S, Green KN, McGaugh JL, LaFerla FM: Intra-neuronal Abeta causes the onset of early Alzheimer's disease-related cognitive deficits in transgenic mice. *Neuron* 2005, 45:675–688
- Neumann M, Sampathu DM, Kwong LK, Truax AC, Micsenyi MC, Chou TT, Bruce J, Schuck T, Grossman M, Clark CM, McCluskey LF, Miller BL, Masliah E, Mackenzie IR, Feldman H, Feiden W, Kretzschmar HA, Trojanowski JQ, Lee VM: Ubiquitinated TDP-43 in frontotemporal lobar degeneration and amyotrophic lateral sclerosis. *Science* 2006, 314:130–133

26. Sampathu DM, Neumann M, Kwong LK, Chou TT, Micsenyi M, Truax A, Bruce J, Grossman M, Trojanowski JQ, Lee VM: Pathological heterogeneity of frontotemporal lobar degeneration with ubiquitin-positive inclusions delineated by ubiquitin immunohistochemistry and novel monoclonal antibodies. *Am J Pathol* 2006, 169:1343–1352
27. Caroni P: Overexpression of growth-associated proteins in the neurons of adult transgenic mice. *J Neurosci Methods* 1997, 71:3–9
28. Guo W, Chen Y, Zhou X, Kar A, Ray P, Chen X, Rao EJ, Yang M, Ye H, Zhu L, Liu J, Xu M, Yang Y, Wang C, Zhang D, Bigio EH, Mesulam M, Shen Y, Xu Q, Fushimi K, Wu JY: An ALS-associated mutation affecting TDP-43 enhances protein aggregation, fibril formation and neurotoxicity. *Nat Struct Mol Biol* 2011, 18:822–830
29. Igaz LM, Kwong LK, Chen-Plotkin A, Winton MJ, Unger TL, Xu Y, Neumann M, Trojanowski JQ, Lee VM: Expression of TDP-43 C-terminal fragments in vitro recapitulates pathological features of TDP-43 proteinopathies. *J Biol Chem* 2009, 284:8516–8524
30. Nonaka T, Kametani F, Arai T, Akiyama H, Hasegawa M: Truncation and pathogenic mutations facilitate the formation of intracellular aggregates of TDP-43. *Hum Mol Genet* 2009, 18:3353–3364
31. Daroszewska A, Ralston SH: Genetics of Paget's disease of bone. *Clin Sci (Lond)* 2005, 109:257–263
32. Buratti E, Baralle FE: Characterization and functional implications of the RNA binding properties of nuclear factor TDP-43, a novel splicing regulator of CFTR exon 9. *J Biol Chem* 2001, 276:36337–36343
33. Buratti E, Brindisi A, Giombi M, Tisminetzky S, Ayala YM, Baralle FE: TDP-43 binds heterogeneous nuclear ribonucleoprotein A/B through its C-terminal tail: an important region for the inhibition of cystic fibrosis transmembrane conductance regulator exon 9 splicing. *J Biol Chem* 2005, 280:37572–37584
34. Kuo PH, Doudeva LG, Wang YT, Shen CK, Yuan HS: Structural insights into TDP-43 in nucleic-acid binding and domain interactions. *Nucleic Acids Res* 2009, 37:1799–1808
35. Wang IF, Wu LS, Chang HY, Shen CK: TDP-43, the signature protein of FTL-D-U, is a neuronal activity-responsive factor. *J Neurochem* 2008, 105:797–806
36. Elvira G, Wasiak S, Blandford V, Tong XK, Serrano A, Fan X, del Rayo Sanchez-Carbente M, Servant F, Bell AW, Boismenu D, Lacaillle JC, McPherson PS, DesGroseillers L, Sossin WS: Characterization of an RNA granule from developing brain. *Mol Cell Proteomics* 2006, 5:635–651
37. Sreedharan J, Blair IP, Tripathi VB, Hu X, Vance C, Rogelj B, Ackerley S, Durnall JC, Williams KL, Buratti E, Baralle F, de Belleruche J, Mitchell JD, Leigh PN, Al-Chalabi A, Miller CC, Nicholson G, Shaw CE: TDP-43 mutations in familial and sporadic amyotrophic lateral sclerosis. *Science* 2008, 319:1668–1672
38. Kabashi E, Valdmanis PN, Dion P, Spiegelman D, McConkey BJ, Vande Velde C, Bouchard JP, Lacomblez L, Pochigaeva K, Salachas F, Pradat PF, Camu W, Meininger V, Dupre N, Rouleau GA: TARDBP mutations in individuals with sporadic and familial amyotrophic lateral sclerosis. *Nat Genet* 2008, 40:572–574
39. Cairns NJ, Neumann M, Bigio EH, Holm IE, Troost D, Hatanpaa KJ, Foong C, White CL 3rd, Schneider JA, Kretschmar HA, Carter D, Taylor-Reinwald L, Paulsmeyer K, Strider J, Gitcho M, Goate AM, Morris JC, Mishra M, Kwong LK, Stieber A, Xu Y, Forman MS, Trojanowski JQ, Lee VM, Mackenzie IR: TDP-43 in familial and sporadic frontotemporal lobar degeneration with ubiquitin inclusions. *Am J Pathol* 2007, 171:227–240
40. Colombrita C, Zennaro E, Fallini C, Weber M, Sommacal A, Buratti E, Silani V, Ratti A: TDP-43 is recruited to stress granules in conditions of oxidative insult. *J Neurochem* 2009, 111:1051–1061
41. Liu-Yesucevitz L, Bilgutay A, Zhang YJ, Vanderweyde T, Citro A, Mehta T, Zaarur N, McKee A, Bowser R, Sherman M, Petrucelli L, Wolozin B: Tar DNA binding protein-43 (TDP-43) associates with stress granules: analysis of cultured cells and pathological brain tissue. *PLoS One* 2010, 5:e13250
42. Ritson GP, Custer SK, Freibaum BD, Guinto JB, Geffel D, Moore J, Tang W, Winton MJ, Neumann M, Trojanowski JQ, Lee VM, Forman MS, Taylor JP: TDP-43 mediates degeneration in a novel *Drosophila* model of disease caused by mutations in VCP/p97. *J Neurosci* 2010, 30:7729–7739
43. Caccamo A, Majumder S, Oddo S: Cognitive decline typical of frontotemporal lobar degeneration in transgenic mice expressing the 25-kDa C-terminal fragment of TDP-43. *Am J Pathol* 2011, 180:293–302
44. Shiina Y, Arima K, Tabunoki H, Satoh J: TDP-43 dimerizes in human cells in culture. *Cell Mol Neurobiol* 2010, 30:641–652
45. Ishigaki S, Hishikawa N, Niwa J, Iemura S, Natsume T, Hori S, Kakizuka A, Tanaka K, Sobue G: Physical and functional interaction between Dornfin and Valosin-containing protein that are colocalized in ubiquitylated inclusions in neurodegenerative disorders. *J Biol Chem* 2004, 279:51376–51385
46. Wojcik C, Rowicka M, Kudlicki A, Nowis D, McConnell E, Kujawa M, DeMartino GN: Valosin-containing protein (p97) is a regulator of endoplasmic reticulum stress and of the degradation of N-end rule and ubiquitin-fusion degradation pathway substrates in mammalian cells. *Mol Biol Cell* 2006, 17:4606–4618
47. Dai RM, Li CC: Valosin-containing protein is a multi-ubiquitin chain-targeting factor required in ubiquitin-proteasome degradation. *Nat Cell Biol* 2001, 3:740–744
48. Kim SH, Shi Y, Hanson KA, Williams LM, Sakasai R, Bowler MJ, Tibbetts RS: Potentiation of amyotrophic lateral sclerosis (ALS)-associated TDP-43 aggregation by the proteasome-targeting factor, ubiquilin 1. *J Biol Chem* 2009, 284:8083–8092
49. Wang X, Fan H, Ying Z, Li B, Wang H, Wang G: Degradation of TDP-43 and its pathogenic form by autophagy and the ubiquitin-proteasome system. *Neurosci Lett* 2010, 469:112–116
50. Wolozin B: Regulated protein aggregation: stress granules and neurodegeneration. *Mol Neurodegener* 2012, 7:56–67
51. McDonald KK, Aulas A, Destroismaisons L, Pickles S, Belec E, Camu W, Rouleau GA, Vande Velde C: TAR DNA-binding protein 43 (TDP-43) regulates stress granule dynamics via differential regulation of G3BP and TIA-1. *Hum Mol Genet* 2011, 20:1400–1410
52. Fiesel FC, Voigt A, Weber SS, Van den Haute C, Waldenmaier A, Gomer K, Walter M, Anderson ML, Kern JV, Rasse TM, Schmidt T, Springer W, Kirchner R, Bonin M, Neumann M, Baekelandt V, Alunni-Fabbroni M, Schulz JB, Kahle PJ: Knockdown of transactive response DNA-binding protein (TDP-43) downregulates histone deacetylase 6. *EMBO J* 2010, 29:209–221
53. Dewey CM, Cenik B, Sephton CF, Dries DR, Mayer P III, Good SK, Johnson BA, Herz J, Yu G: TDP-43 is directed to stress granules by sorbitol, a novel physiological osmotic and oxidative stressor. *Mol Cell Biol* 2011, 31:1098–1108
54. Parker SJ, Meyerowitz J, James JL, Liddell JR, Crouch PJ, Kanninen KM, White AR: Endogenous TDP-43 localized to stress granules can subsequently form protein aggregates. *Neurochem Int* 2012, 60:415–424
55. Weihl CC, Miller SE, Hanson PI, Pestronk A: Transgenic expression of inclusion body myopathy associated mutant p97/VCP causes weakness and ubiquitinated protein inclusions in mice. *Hum Mol Genet* 2007, 16:919–928